Nanoscale

Accepted Manuscript

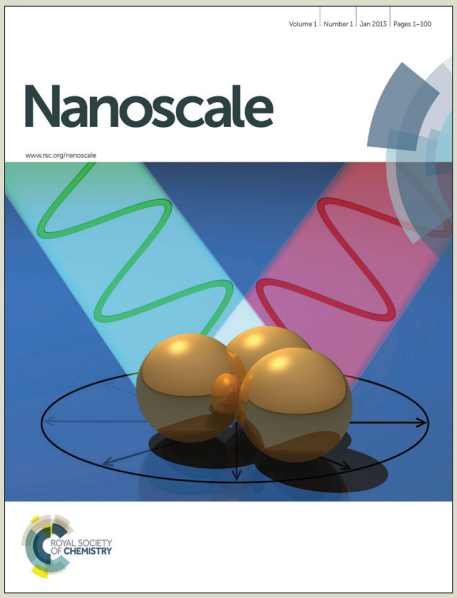

Journal Name

COMMUNICATION

Metal Diselenide Nanoparticles as Highly Active and Stable Electrocatalyst for Hydrogen Evolution Reaction

Received 00th January 20xx,
Accepted 00th January 20xx

DOI: 10.1039/x0xx00000x

www.rsc.org/

Jia Liang,[a,b] Yingchao Yang,[a] Jing Zhang,[a] Jingjie Wu,[a] Pei Dong,[a] Jiangtan Yuan,[a] Gengmin Zhang[b] and Jun Lou[*,a]

In this communication, Nickel diselenide ($NiSe_2$) nanoparticles are synthesized by a facile and low-cost hydrothermal method. The synthesis method can be extended to other metal diselenides as well. The electrode made of $NiSe_2$ exhibits superior electrocatalytic activity in hydrogen evolution reaction (HER). A low Tafel slope of 31.1 mV/decade is achieved for $NiSe_2$, which is comparable to that of Platinum (~30 mV/decade). Moreover, the catalytic activity of $NiSe_2$ is very stable and no obvious degradation is found even after 1000 cyclic voltammetric sweeps.

The discovery and development of advanced non-noble metal materials for electrocatalytic water-splitting has been driven by society's needs for clean energy. Hydrogen has been regarded as an ideal chemical fuel for sustainable energy application owing to its highest specific energy.[1-3] Among various routes to obtain pure hydrogen, the electrochemical hydrogen evolution reaction (HER) attracts broad attentions.[4] However, platinum (Pt) as the most active HER catalyst is expensive and scarce, which makes it unsuitable for large scale hydrogen production. Therefore, it remains challenging to search for alternative Pt-free HER catalysts based on low-cost and acid-stable materials.

Recently, a number of potential earth-abundant materials have emerged as Pt substitute for HER catalysts, including MoS_2,[5-11] $MoSe_2$,[12-13] Mo_2C,[14-16] WS_2,[17] WSe_2,[13] W_2C,[18-19] WC,[20] $NiMoN_x$,[21] $Co_{0.6}Mo_{1.4}N_2$,[22] CoS[23] and Co_3O_4[24]. Several groups also demonstrated that transition metal dichalcogenides synthesized by sulfurization/selenization of metal films using chemical vapor deposition (CVD) or electron beam deposition (EBD) can be used as high-performance HER catalysts.[25-26] However, it is impractical to use these methods to fabricate and deploy HER catalysts in large scale because of their high cost and limited production yield in such procedures.

On the other hand, Nickel (Ni), as an earth abundant element, is considered to be one of the most promising HER catalyst materials. A multitude of Ni-based materials have been prepared and their activities for HER were measured. For example, Ni-based thin films,[27] Ni-Mo nanopowders,[28] Ni-Mo-N_x nanosheets,[21] raney Ni-Sn,[29] and Ni-Al particles[30]. However, due to their poor corrosion resistance, most of these Ni-based catalysts have the issue of instability in acidic electrolytes. In this study, we have developed Nickel diselenide ($NiSe_2$) nanoparticles with octahedron morphology and their HER performances in acidic electrolyte have been investigated. The results show that $NiSe_2$ catalyst exhibits an excellent activity for HER and extremely high electrochemical stability in acidic electrolyte even after 1000 cyclic voltammetric (CV) cycles.

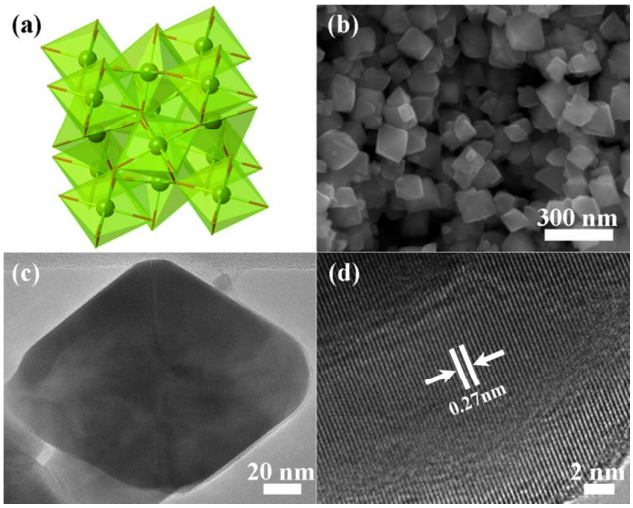

Fig. 1 (a) Crystal structure of pyrite-type; SEM (b), TEM (c), and HRTEM (d) images of $NiSe_2$ nanoparticles.

The $NiSe_2$ catalyst was synthesized by a facile and low-cost hydrothermal method using $NiCl_2{\cdot}6H_2O$ as the precursor (See detailed experimental methods, Supporting Information). $NiSe_2$ possesses a pyrite structure, in which the Ni atoms are octahedrally bonded to adjacent selenium atoms, as shown in Fig. 1a.[31-32] Fig. 1b shows a typical scanning electron microscopy (SEM) image of $NiSe_2$ nanoparticles with the size in the range of 100–150 nm. Most $NiSe_2$

[a.] Department of Materials Science and NanoEngineering, Rice University, 6100 Main Street, Houston, Texas 77005, United States
[b.] Key Laboratory for the Physics and Chemistry of Nanodevices and Department of Electronics, Peking University, Beijing 100871, China
† Electronic Supplementary Information (ESI) available: [Experimental Section, additional Figures and Tables]. See DOI: 10.1039/x0xx00000x

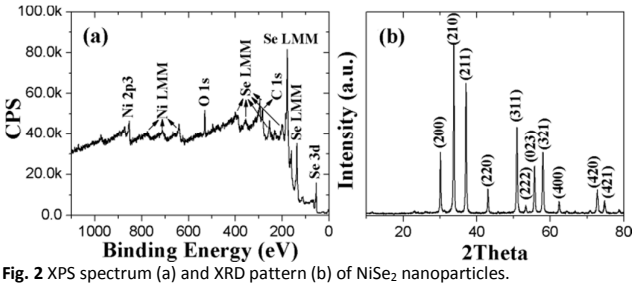

Fig. 2 XPS spectrum (a) and XRD pattern (b) of $NiSe_2$ nanoparticles.

nanoparticles display an octahedral structure, which can be attributed to the effect of the crystal habit on the morphology.[33-34] To reveal the microstructure of $NiSe_2$ nanoparticles, transmission electron microscopy (TEM) and high-resolution TEM (HRTEM) studies were performed. Fig. 1c illustrates a selected $NiSe_2$ nanoparticle with octahedral structure, which is consistent with the SEM observations (Fig. 1b). Fig. 1d reveals a HRTEM image of a $NiSe_2$ nanoparticle. The distance between lattice fringes, 0.27 nm, is assigned to (210) planes of the $NiSe_2$ (JCPDS card: 65-1843), suggesting that the $NiSe_2$ nanoparticles are well-crystallized. It should be noted that such synthetic strategy is also suitable for other metal dichalcogenides, namely, $CoSe_2$ and $PdSe_2$, when the $NiCl_2{\cdot}6H_2O$ is replaced by their corresponding precursors of $CoSO_4{\cdot}7H_2O$ and $PdCl_2$, respectively. The SEM and TEM images of $CoSe_2$ and $PdSe_2$ are exhibited in Fig. S1.

Fig. 2a shows the X-ray photoelectron spectroscopy (XPS) spectrum of $NiSe_2$ nanoparticles. The spectrum is dominated by the photoelectron lines of Ni and Se elements. The C 1s line is also found in the spectrum because of the carbon in the atmosphere. The C 1s line is used as the standard for calibration during our data processing. The peaks assigned to Ni $2p_{3/2}$, Se $3d_{3/2}$, and Se $3d_{5/2}$ are detected at 853.1 eV, 55.2 eV, and 54.6 eV, respectively, which are consistent with $NiSe_2$ in previous works.[33-34] This result is also confirmed by the energy dispersive X-ray spectroscopy (EDX) study shown in Fig. S2 (Supporting Information), which shows a 16:33 Ni:Se ratio. Fig. 2b shows the X-ray diffraction (XRD) pattern of $NiSe_2$ nanoparticles. All the diffraction peaks are consistent with the JCPDS card 65-1843, which is in agreement with the TEM results (Fig. 1d). No other impurities can be found from the XPS and XRD results, indicating that $NiSe_2$ nanoparticles fabricated by this hydrothermal method are with extremely high purity. Similarly, the XPS and EDX results of $CoSe_2$ and $PdSe_2$ obtained using the same synthetic strategy can be found in Figs. S3 and S4 (Supporting Information).

The HER catalytic activities of $NiSe_2$, $CoSe_2$, and $PdSe_2$ nanoparticles were measured using the standard three-electrode electrochemical cell setup in 0.5 M H_2SO_4. The working electrodes were prepared by depositing the inks of $NiSe_2$, $CoSe_2$, and $PdSe_2$ on glassy carbons, respectively, yielding a mass loading of ~1 mg/cm^2 (See detailed Electrochemical measurements, Supporting Information). Electrochemical impedance spectroscopy in Fig. S5 reveals small ohmic resistances (~ 8Ω) for these three working electrodes. All of the data in this report have been iR-corrected by subtracting the ohmic resistance loss from the overpotential. Fig. 3a shows the polarization curves displaying the current density vs. voltage (j vs. V) of the Pt/C, $NiSe_2$, $CoSe_2$, and $PdSe_2$ catalysts. For the $NiSe_2$, $CoSe_2$, and $PdSe_2$ catalysts, more than 5 electrodes were

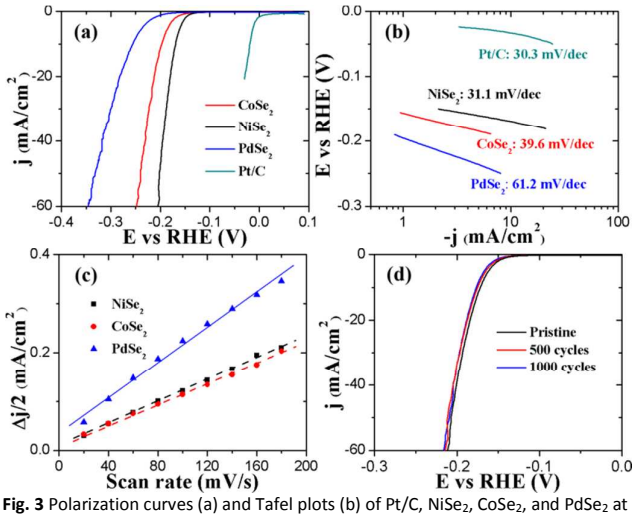

Fig. 3 Polarization curves (a) and Tafel plots (b) of Pt/C, $NiSe_2$, $CoSe_2$, and $PdSe_2$ at a scan rate of 5 mV/s; (c) Linear fitting of the capacitive current density of $NiSe_2$, $CoSe_2$, and $PdSe_2$ *vs* scan rate; (d) Polarization curves of $NiSe_2$ before and after 500 or 1000 CV cycles for stability test.

tested and their HER activities were highly consistent, as shown in Fig. S6 and Table S1. The overpotentials required for $NiSe_2$, $CoSe_2$, and $PdSe_2$ to produce the cathodic current density of 10 mA/cm^2 are 170, 196, and 255 mV, respectively, as shown in Table S2. Clearly, $NiSe_2$ exhibits the highest HER catalytic activity among the three catalysts. Compared with other non-noble catalytic materials, the overpotential of $NiSe_2$ is quite outstanding, as shown in Table S2. These non-noble catalytic materials possess the overpotential ranged from 100 to 250 mV at the cathodic current densties of 0.1-20 mA/cm^2. Among them, Ni-Mo nanopowders exhibit better catalytic activity than $NiSe_2$, but the activity of Ni-Mo nanopowders degrade rapidly in acidic conditions.[28] The reported $NiSe_2$ and Li-MoS_2 synthesized by CVD method exhibit a higher initial activity than the $NiSe_2$ nanoparticles in this work, but the loading amounts in their working electrodes are almost twice and four times as much, respectively. Moreover, the selenization/sulfuration process using CVD method is likely too costly and inefficient to be employed for large scale applications.[25,35] Without considering the cost, figure 3a also shows the catalytic performance of Pt/C catalyst, which shows a highly active catalytic activity for the HER and is in accordance with previous literature.

Fig. 3b shows the corresponding Tafel plots of the Pt/C, $NiSe_2$, $CoSe_2$, and $PdSe_2$ catalysts. The linear portions of the Tafel plot are fit to the Tafel equation ($\eta = b\log(j) + a$, where b is the Tafel slope), yielding Tafel slopes of 30.3, 31.1, 39.6, and 61.2 mV/dec for Pt/C, $NiSe_2$, $CoSe_2$, and $PdSe_2$ catalysts, respectively. Notably, the small Tafel slope for $NiSe_2$ is comparable with that of Pt/C catalyst, which is desirable to prompt a large catalytic current density at low overpotential. Compared with the Tafel slopes of other non-noble metal catalytic materials like MoS_2 (40~60 mV/dec),[6,35] $MoSe_2$ (59.8 mV/dec),[13] and $NiMoN_x$ (35.9 mV/dec),[21] the lower Tafel slope of our $NiSe_2$ shows better catalytic performance. Even for the same materials of $NiSe_2$ fabricated by CVD method,[25] $NiSe_2$ synthesized in this report by hydrothermal method still exhibits lower Tafel slope. Exchange current density, another crucial parameter for HER activity, is also obtained when fitting the Tafel plot to the Tafel equation, as shown in Table S2. The exchange current densities for

$NiSe_2$ and $CoSe_2$ are almost the same, and $PdSe_2$ has the biggest exchange current density (6.6×10^{-4} mA/cm^2). However, the Tafel slope of $PdSe_2$ is much larger than those of $NiSe_2$ and $CoSe_2$, demonstrating worse catalytic performance towards HER.

Effective surface area is another important factor for HER catalytic activities. The effective surface area is expected to be linearly proportional to the electrochemical double layer capacitance. Therefore, an alternative approach to estimate the relative effective surface area for the $NiSe_2$, $CoSe_2$, and $PdSe_2$ catalysts is to measure the electrochemical double layer capacitance using a simple cyclic volatammetry (CV) method, as shown in Fig. S7. The electrochemical double layer capacitances can be estimated from the slopes of the curves as shown in Fig. 3c, which is the halves of the positive and negative current density differences at the center of the potential ranges vs. the voltage scan rates. Clearly, the $PdSe_2$ catalyst has the highest capacitance and the $NiSe_2$ and $CoSe_2$ catalysts possess almost the same capacitance, which is in agreement with the results of the exchange current density.[25] Combining the low catalytic performance and high surface area, the $PdSe_2$ catalyst does have poorer intrinsic activity toward HER compared with the other two catalysts of $NiSe_2$ and $CoSe_2$. Considering all the factors, the small Tafel slope and relative large exchange current density confirm that $NiSe_2$ is among the best catalytic non-noble materials.

For heterogeneous catalysts, their catalytic activities were mostly dependent on the reactive states near Fermi level.[26] In metal diselenide, the density of states in the conduction band mainly resulted from d-electron filling in e_g orbital. Meanwhile, the e_g band was partially filled for the $NiSe_2$ and $CoSe_2$ catalysts.[26,36-38] Thus, the excellent activities of $NiSe_2$ and $CoSe_2$ catalysts were likely due to their unique electronic structures.[26] Moreover, as we know, different morphologies of the catalysts have some influences on the catalytic performances due to their distinct crystal facets.[39-40] As shown in Figure 1 and Figure S1, $NiSe_2$ shows a more uniform morphology, which may possess favorable crystal facets for a high HER performance, than $CoSe_2$. Therefore, the former reveals the better catalytic activity than the latter.

To evaluate the stability of the $NiSe_2$ catalyst during electrocatalytic hydrogen revolution in 0.5 M H_2SO_4, the polarization curves after 500 and 1000 cycles CV sweeps are shown in Fig. 3d. Polarization curves after 500 and 1000 cycles almost overlay on top of the pristine curve before CV sweeps. Specifically, the overpotentials required for $NiSe_2$ after 500 and 1000 cycles to produce the cathodic current density of 10 mA/cm^2 are 174 and 176 mV, respectively, which is very close to the pristine value of 170 mV. It confirms that, unlike most other Ni-based HER catalytic materials with instability in acidic solution, the $NiSe_2$ catalyst is stable in acidic solution and intact even undergoing repeated cycling. Moreover, for the $NiSe_2$ catalyst, the cathodic current density as a function of the reaction time at the fixed overpotential of -170 mV (after *iR* correction) was measured, as shown in Fig. S8. This result reveals that the cathodic current density for the $NiSe_2$ catalyst displays a negligible degradation after 3 h testing at the fixed overpotential. That is, this curve further demonstrates that the $NiSe_2$ catalyst possesses excellent stability in acidic solution. Similarly, the $CoSe_2$, and $PdSe_2$ catalysts also exhibit the highly stable catalytic activities in the strongly acidic condition, as shown in Fig. S9.

Conclusions

In conclusion, we synthesized $NiSe_2$ nanoparticles by a facile and low-cost hydrothermal method. Other homological metal dichalcogenides of $CoSe_2$ and $PdSe_2$ were also fabricated using the same synthetic strategy. We next evaluated them as electrocatalysts for the hydrogen evolution reaction under strong acidic conditions. The electrode consists of $NiSe_2$ exhibited excellent electrocatalytic activity with a Tafel slope as small as 31.1 mV/decade, which is comparable with that of platinum. In addition, the catalytic activity of $NiSe_2$ was almost unchanged after 1000 cyclic voltammetric sweeps, confirming its long-term durability under acidic conditions.

Acknowledgements

The authors would like to acknowledge the support from the Welch Foundation grant C-1716.

Notes and references

1 M. S. Dresselhaus, I. L. Thomas, *Nature* 2001, **414**, 332.
2 J. A. Turner, *Science* 2004, **305**, 972.
3 J. Zhang, L. F. Qi, J. R. Ran, J. G. Yu, S. Z. Qiao, *Adv. Energy Mater.* 2014, **4**, 1301925.
4 M. G. Walter, E. L. Warren, J. R. McKone, S. W. Boettcher, Q. Mi, E. A. Santori, N. S. Lewis, *Chem. Rev.* 2010, **110**, 6446.
5 J. Kibsgaard, Z. Chen, B. N. Reinecke, T. F. Jaramillo, *Nat. Mater.* 2012, **11**, 963.
6 T. F. Jaramillo, K. P. Jorgensen, J. Bonde, J. H. Nielsen, S. Horch, I. Chorkendorff, *Science* 2007, **317**, 100.
7 H. Wang, Z. Lu, S. Xu, D. Kong, J. J. Cha, G. Zheng, P. C. Hsu, K. Yan, D. Bradshaw, F. B. Prinz, Y. Cui, *Proc. Natl. Acad. Sci. USA* 2013, **110**, 19701.
8 Y. Li, H. Wang, L. Xie, Y. Liang, G. Hong, H. Dai, *J. Am. Chem. Soc.* 2011, **133**, 7296.
9 B. Hinnemann, P. G. Moses, J. Bonde, K. P. Jorgensen, J. H. Nielsen, S. Horch, I. Chorkendorff, J. K. Norskov, *J. Am. Chem. Soc.* 2005, **127**, 5308.
10 M. A. Lukowski, A. S. Daniel, F. Meng, A. Forticaux, L. Li, S. Jin, *J. Am. Chem. Soc.* 2013, **135**, 10274.
11 D. Voiry, M. Salehi, R. Silva, T. Fujita, M. W. Chen, T. Asefa, V. B. Shenoy, G. Eda, M. Chhowalla, *Nano Lett.* 2013, **13**, 6222.
12 D. Kong, H. Wang, J. J. Cha, M. Pasta, K. J. Koski, J. Yao, Y. Cui, *Nano Lett.* 2013, **13**, 1341.
13 H. Wang, D. Kong, P. Johanes, J. J. Cha, G. Zheng, K. Yan, N. Liu, Y. Cui, *Nano Lett.* 2013, **13**, 3426.
14 H. Vrubel, X. Hu, *Angew. Chem., Int. Ed.* 2012, **51**, 12703.
15 W. F. Chen, C. H. Wang, K. Sasaki, N. Marinkovic, W. Xu, J. T. Muckerman, R. R. Adzic, *Energy Environ. Sci.* 2013, **6**, 943.
16 L. Liao, S. Wang, J. Xiao, X. Bian, Y. Zhang, M. D. Scanlon, X. Hu, B. Liu, H. H. Girault, *Energy Environ. Sci.* 2014, **7**, 387.
17 D. Voiry, H. Yamaguchi, J. Li, R. Silva, D. C. B. Alves, T. Fujita, M. Chen, T. Asefa, V. B. Shenoy, G. Eda, M. Chhowalla, *Nat. Mater.* 2013, **12**, 850.
18 D. J. Ham, R. Ganesan, J. S. Lee, *Int. J. Hydrogen Energ.* 2008, **33**, 6865.
19 F. Harnisch, G. Sievers, U. Schroeder, *Appl. Catal. B: Environ.* 2009, **89**, 455.

20 A. T. Garcia-Esparza, D. Cha, Y. Ou, J. Kubota, K. Domen, K. Takanabe, *Chemsuschem* 2013, **6**, 168.
21 W. F. Chen, K. Sasaki, C. Ma, A. I. Frenkel, N. Marinkovic, J. T. Muckerman, Y. Zhu, R. R. Adzic, *Angew. Chem., Int. Ed.* 2012, **51**, 6131.
22 B. Cao, G. M. Veith, J. C. Neuefeind, R. R. Adzic, P. G. Khalifah, *J. Am. Chem. Soc.* 2013, **135**, 19186.
23 Y. Sun, C. Liu, D. C. Grauer, J. Yano, J. R. Long, P. Yang, C. J. Chang, *J. Am. Chem. Soc.* 2013, **135**, 17699.
24 Y. C. Wang, T. Zhou, K. Jiang, P. M. Da, Z. Peng, J. Tang, B. Kong, W. B. Cai, Z. Q. Yang, G. F. Zheng, *Adv. Energy Mater.* 2014, **4**, 1400696.
25 D. Kong, H. Wang, Z. Lu, Y. Cui, *J. Am. Chem. Soc.* 2014, **136**, 4897.
26 D. Kong, J. J. Cha, H. Wang, H. R. Lee, Y. Cui, *Energy Environ. Sci.* 2013, **6**, 3553.
27 C. He,; X. Wu, Z. He, *J. Phys. Chem. C* 2014, **118**, 4578.
28 J. R. McKone, B. F. Sadtler, C. A. Werlang, N. S. Lewis, H. B. Gray, *Acs Catal.* 2013, **3**, 166.
29 G. W. Huber, J. W. Shabaker, J. A. Dumesic, *Science* 2003, **300**, 2075.
30 J. Dulle, S. Nemeth, E. V. Skorb, T. Irrgang, J. Senker, R. Kempe, D. V. Andreeva, *Adv. Funct. Mater.* 2012, **22**, 3128.
31 H. Fan, M. Zhang, X. Zhang, Y. Qian, *J. Cryst. Growth* 2009, **311**, 4530.
32 V. H. McCann, J. B. Ward, *J. Phys. Chem. Solids* 1977, **38**, 991.
33 Z. H. Han, S. H. Yu. Y. P. Li, H. Q. Zhao, F. Q. Li, Y. Xie, Y. T. Qian, *Chem. Mater.* 1999, **11**, 2302.
34 J. Yang, G. H. Cheng, J. H. Zeng, S. H. Yu, X. M. Liu, Y. T. Qian, *Chem. Mater.* 2001, **13**, 848.
35 H. Wang, Z. Y. Lu, D. Kong, J. Sun, T. M. Hymel, Y. Cui, *ACS Nano* 2014, **8,** 4940.
36 S. Ogawa, *J. Appl. Phys.* 1979, **50,** 2308.
37 J. K. Norskov, F. Abild-Pedersen, F. Studt, T. Bligaard, *Proc. Natl. Acad. Sci.* 2011, **108,** 937.
38 A. Vojvodic, J. K. Norskov, *Science* 2011, **334,** 1355.
39 Q. L. Yao, M. Huang, Z. H. Lu, Y. W. Yang, Y. X. Zhang, X. S. Chen, Z. Yang, *Dalton Trans.* 2015, **44,** 1070.
40 G. L. Li, J. Yuan, B. Y. Han, W. F. Shangguan, *Int. J. Hydrogen Energy* 2011, **36,** 4271.